Diagn Interv Radiol 2008; 14:147-152

ORIGINAL ARTICLE

MRI findings in parosteal osteosarcoma: correlation with histopathology

Fuldem Yıldırım Dönmez, Ümit Tüzün, Ceyla Başaran, Mehtap Tunacı, Bilge Bilgiç, Gülden Acunaş

PURPOSE
To assess the role of magnetic resonance imaging (MRI), particularly signal intensity changes, in predicting the dedifferentiation of parosteal osteosarcoma, and to evaluate other factors that may affect grading on MRI.

MATERIALS AND METHODS
MRI of 12 patients with parosteal osteosarcoma diagnosed on plain radiography were reviewed with regard to size, location, extent, soft tissue component, intramedullary invasion, and signal characteristics. The findings are correlated with histopathologic results.

RESULTS
By histopathological examination there were 6 Grade I, 3 Grade II, and 3 Grade III tumors. Average size was 11 cm. All cases had a soft tissue component. Intramedullary extension was evident in 3/6 of the Grade I cases, 2/3 of the Grade II cases, and all (3/3) of the Grade III cases. T1-weighted images revealed lesions of marked hypointensity. Signal intensity on T2-weighted images varied with the presence of necrosis and hemorrhage in relation to size, regardless of the grade of the tumor. Contrast-enhanced images revealed enhancement of the solid components; no enhancement was observed in the necrotic or hemorrhagic parts.

CONCLUSION
High and heterogeneous signal on T2-weighted images of Grade I, II, and III tumors is not specific for the dedifferentiated component, due to hemorrhage and necrosis in large masses. Therefore, high signal intensity on T2-weighted images is not always a reliable way to predict the grade of the tumor. Contrast enhanced T1-weighted images can be valuable to show the solid component in the heterogeneous areas on T2-weighted images, and can be useful in guiding the biopsy.

Key words: • *parosteal osteosarcoma* • *magnetic resonance imaging* • *surface osteosarcoma* • *dedifferentiation*

From the Department of Radiology (F.Y.D. ✉ *fuldemyildirim@yahoo.com*, C.B.), Başkent University School of Medicine, Ankara, Turkey; the Departments of Radiology (Ü.T., M.T., G.A.), and Pathology (B.B.), İstanbul University School of Medicine, İstanbul, Turkey.

Received 19 October 2007; revision requested 21 April 2008; revision received 25 April 2008; accepted 28 April 2008.

Parosteal osteosarcoma is an uncommon variant of osteosarcoma, arising from the juxtacortical areas of the long bones (1). Parosteal osteosarcoma is the least malignant of the osteogenic tumors, and typically carries a relatively good prognosis. Often, it is curable if the neoplasm is detected when there is not significant extension into the medullary cavity (2). It is generally a low-grade tumor; however, it may occasionally dedifferentiate into high-grade sarcoma, which has a significantly worse prognosis, similar to that of patients with conventional osteosarcoma (3). Therefore histologic grade is the most important factor in predicting the clinical behaviour of parosteal osteosarcoma.

Radiologically, parosteal osteosarcoma usually presents as a lobulated, dense bony mass, with a radiolucent line that appears to separate the dense bony mass of the tumor from the bone cortex (4). Computed tomography (CT) accurately defines the extent of the tumor for surgical planning, however it does not always reveal the presence of medullary invasion (5). Magnetic resonance imaging (MRI) is clearly superior to other imaging methods for early detection of bone marrow involvement (2). Jelinek et al. described the features on CT and MRI to predict the histologic grade in their study, which concluded that a poorly defined soft tissue component distinct from the ossified matrix is the most diagnostic feature of high-grade parosteal osteosarcoma (6).

In this study, we report our own observations in 12 patients with parosteal osteosarcoma, and assess the role of MRI, particularly the role of signal intensity changes, in predicting the histologic grade and dedifferentiation of parosteal osteosarcoma. In addition, we evaluate with MRI other factors that may affect grading, and investigate how MRI can be useful for patients with parosteal osteosarcoma.

Materials and methods

MRI studies were reviewed on 12 patients (2 males and 10 females) who had histologically proven parosteal osteosarcoma and were admitted to our orthopedic oncology center between 1990 and 2005.

The patients ranged in age from 17 to 54 years (mean age, 33 years). The locations of the tumors were the distal end (n = 8) and proximal end (n = 2) of the femur, and the proximal end of the humerus (n = 1) and tibia (n = 1).

Ten patients were admitted to the hospital with a palpable mass. Of the other two patients, one presented with swelling, and the other, with knee pain. Duration of symptoms ranged from 1 month to 3 years. No patient had a prior history of trauma. All tumors were widely resected on the 12th to the 23rd day (mean, 14 days) after MRI.

MRI studies were performed with dedicated extremity coils utilizing 1-1.5 T scanners (Siemens Magnetom™ and Siemens Symphony, Siemens Medical Systems, Erlangen, Germany). Imaging protocols included T1-

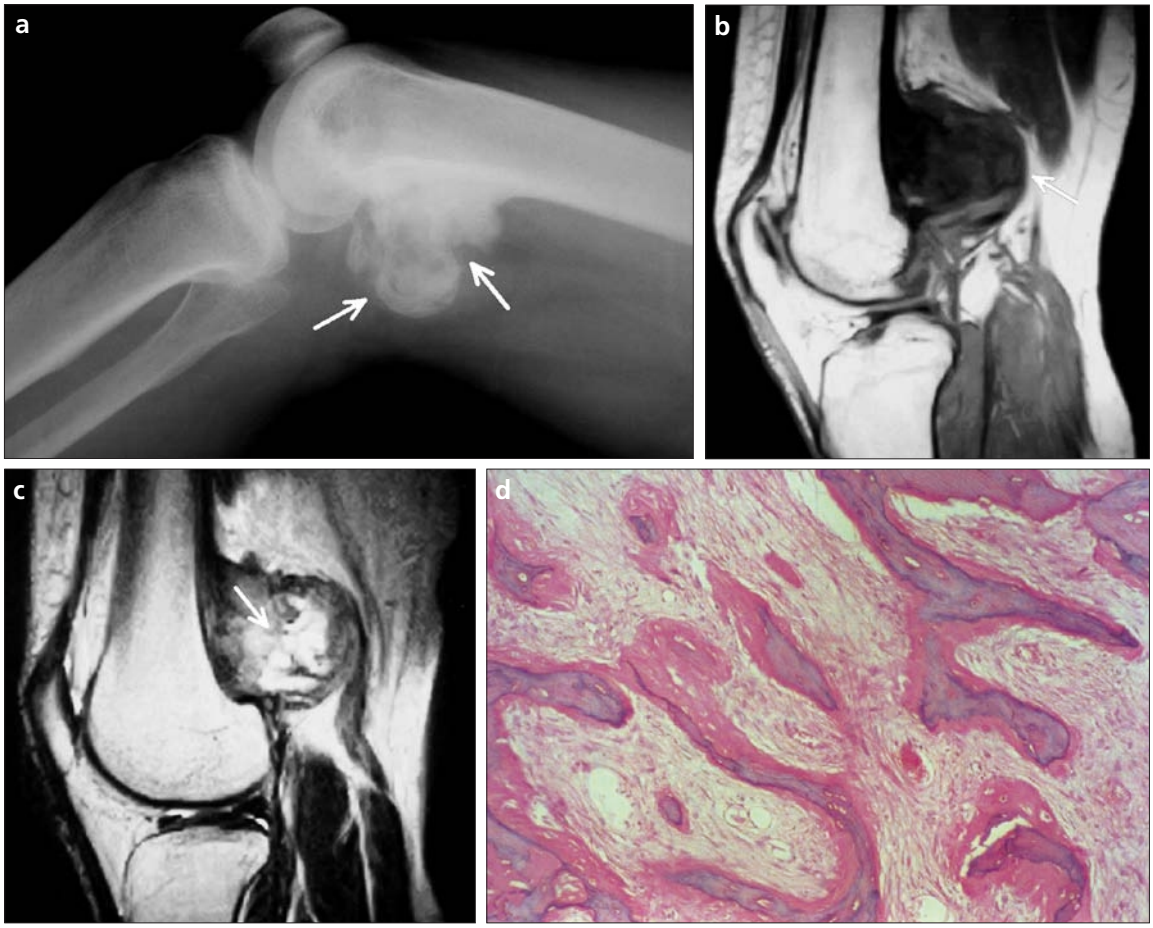

Figure 1. a–d. Grade I parosteal osteosarcoma. Lateral radiograph of the knee **(a)** shows an ossified mass on the dorsal aspect of the femur *(arrows)*. On T1-weighted sagittal MR image **(b)**, a round hypointense mass originating from the posterior aspect of the femur is seen *(arrow)*. T2-weighted sagittal MR image **(c)** shows the hyperintense signal intensity of the tumor due to hemorrhage *(arrow)*. Histopathologically, irregular lamellar bone formation and spindle-cell infiltration is evident (**d**, HE x125).

weighted spin echo (TR/TE, 515–650/10–16 ms) with and without IV gadolinium (Magnevist, Schering, Berlin, Germany) (in 6 patients), T2-weighted spin echo (TR/TE, 3800–5000/80–120 ms) with or without fat saturation in at least two orthogonal planes.

MR images were analyzed by two musculoskeletal radiologists who had full knowledge of the pathology results, and final interpretation was established by consensus. MRI features that were analyzed included the bones involved, location, size, shape, and margins of the tumor, as well as signal characteristics on T1-weighted and T2-weighted sequences, presence of cleavage plane, soft tissue component, and intramedullary invasion. The longest diameter was measured for establishment of tumor size. Signal intensity was compared with that of normal skeletal muscle on both T1-weighted and T2-weighted images, and described as hypointense, isointense, hyperintense, and heterogeneous. Intramedullary invasion was defined as the involvement of the medullary component, visible on all sequences.

The biopsies were performed immediately after the MRI examination and with attention to MRI findings, prior to surgery. Biopsies were taken from 3 different locations, with the guidance of contrast-enhanced images, including both enhanced and unenhanced areas.

Each case was evaluated by a pathologist with 15 years of experience in musculoskeletal pathology. Histologic grading was described as follows: Grade I: hypocellular stroma with subtle atypia; Grade II: mild increase in stromal cellularity and more prominent cytologic atypia; Grade III: marked pleomorphism with high cytologic atypia and high mitotic rate, also called dedifferentiated type. Duration of the clinical follow-up varied from 1 to 15 years.

This retrospective study was approved by the institutional review board.

Results

According to the histopathological examination, 6 of the tumors were Grade I (low) (Fig. 1), 3 were Grade II (intermediate) (Fig. 2) and 3 were Grade III (high, dedifferentiated) (Fig. 3). One of each grade was a recurrent tumor. The recurrent Grade II and Grade III tumors were Grade I at initial diagnosis.

The overall tumor sizes ranged between 4.5 cm and 25 cm at their greatest long axis (mean, 11 cm). The average sizes were 11.3 cm, 6.6 cm, and 14.5 cm for Grade I, Grade II and Grade III tumors, respectively. For each case, clinical details, MR signal intensity, histopathological grade of the tumor, and presence of hemorrhage and necrosis are tabulated in Table. Grade I tumors had well-defined borders, whereas high-grade lesions were

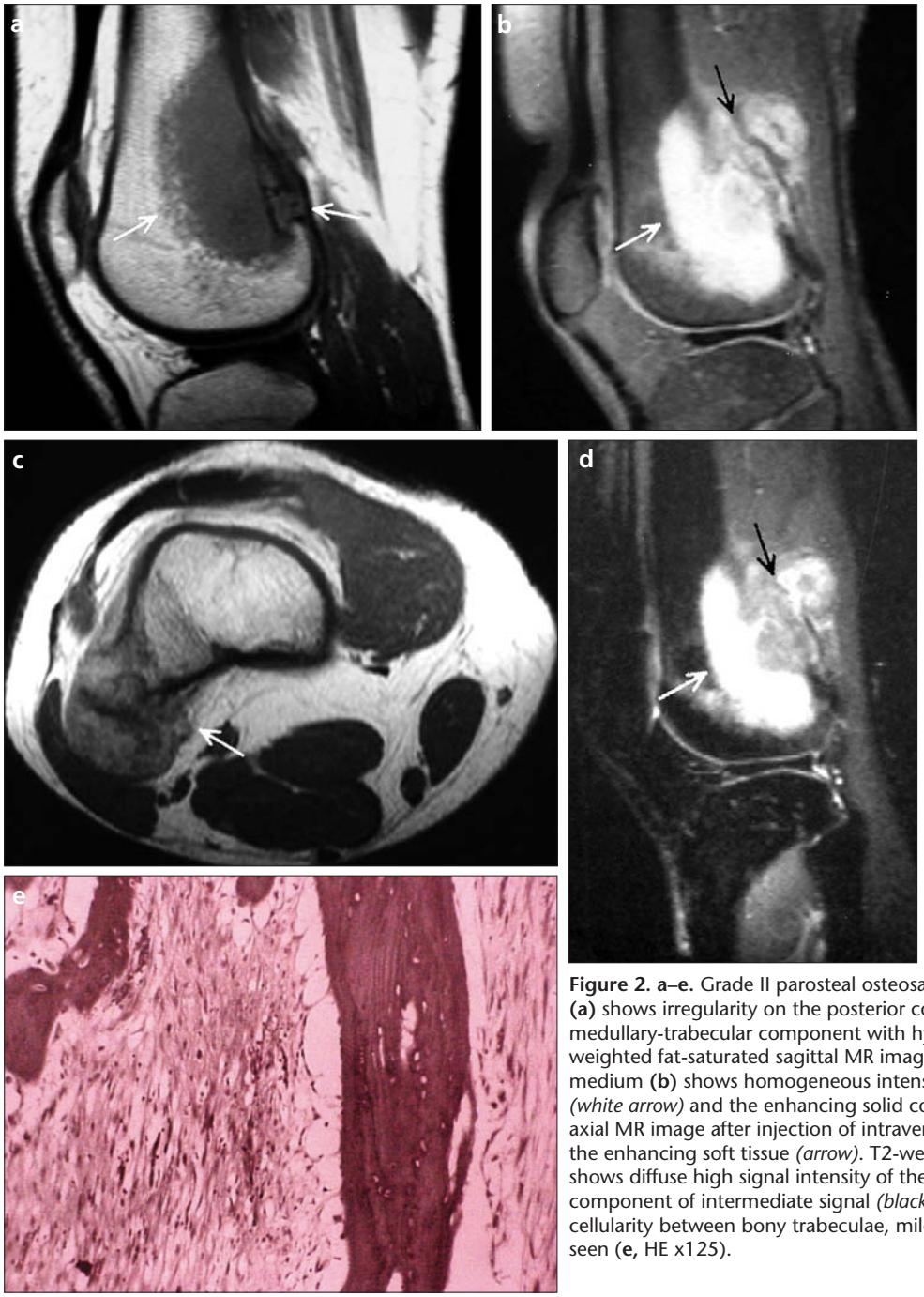

Figure 2. a–e. Grade II parosteal osteosarcoma. T1-weighted sagittal MR image **(a)** shows irregularity on the posterior cortex of the femur and invasion of the medullary-trabecular component with hypointense signal intensity *(arrows)*. T1-weighted fat-saturated sagittal MR image after injection of intravenous contrast medium **(b)** shows homogeneous intense enhancement of the medullary cavity *(white arrow)* and the enhancing solid component *(black arrow)*. T1-weighted axial MR image after injection of intravenous contrast medium **(c)** shows the enhancing soft tissue *(arrow)*. T2-weighted fat-saturated MR image **(d)** shows diffuse high signal intensity of the marrow *(white arrow)* and the solid component of intermediate signal *(black arrow)*. Histopathologically, moderate cellularity between bony trabeculae, mild pleomorphic spindle cell infiltration is seen (**e,** HE x125).

ill-defined, large masses. There was a soft tissue component in all cases, with no cleavage plane between the tumor and the soft tissue. Intramedullary extension was evident in 3 of 6 Grade I cases, 2 of 3 Grade II cases, and all 3 Grade III cases.

T1-weighted images revealed lesions of marked hypointensity compared with normal skeletal muscle. Signal intensity on T2-weighted images varied depending on the presence of necrosis and hemorrhage. Most commonly, there was heterogeneous signal on T2-weighted images on all three grades of tumors (4 of 6 Grade I, 2 of 3 Grade II, and all of Grade III tumors), especially when the tumor was large. The histopathologic findings on biopsy were directly compared with contrast-enhanced MRI findings, revealing enhancement of the solid components; however, no enhancement was observed in some areas, which were found to be necrotic or hemorrhagic on histopathological examination.

Discussion

Usually a low-grade malignancy with little potential for metastasis, parosteal osteosarcoma is the most common subtype of surface osteosarcomas, accounting for over 75% of all surface osteosarcomas. There is a female predominance, and the peak age of presentation is in the second or third decade. The tumor occurs almost exclusively in long tubular bones, although there are a few published case reports of parosteal osteosarcomas in the axial

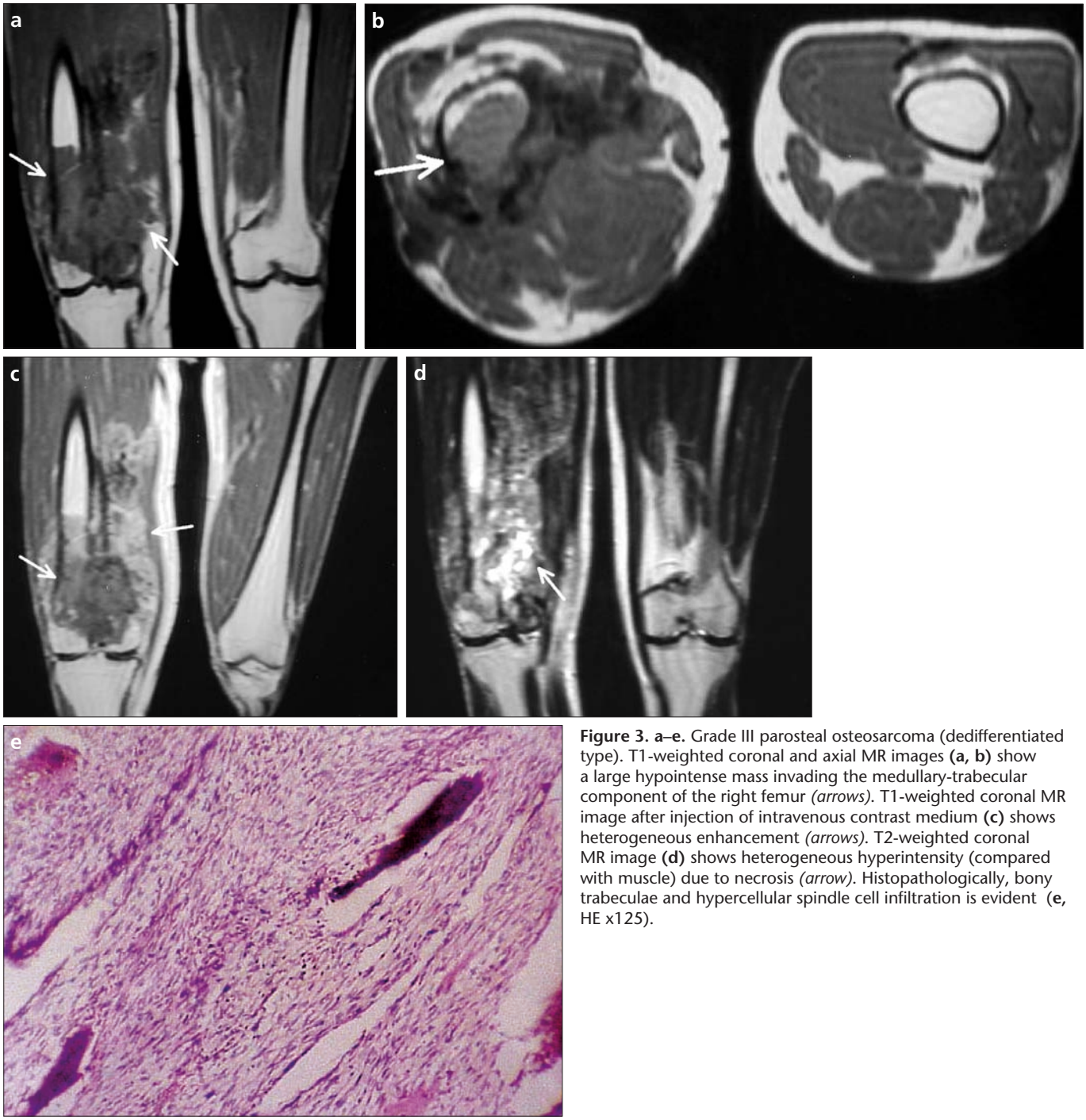

Figure 3. a–e. Grade III parosteal osteosarcoma (dedifferentiated type). T1-weighted coronal and axial MR images **(a, b)** show a large hypointense mass invading the medullary-trabecular component of the right femur *(arrows)*. T1-weighted coronal MR image after injection of intravenous contrast medium **(c)** shows heterogeneous enhancement *(arrows)*. T2-weighted coronal MR image **(d)** shows heterogeneous hyperintensity (compared with muscle) due to necrosis *(arrow)*. Histopathologically, bony trabeculae and hypercellular spindle cell infiltration is evident **(e,** HE x125).

skeleton. The most common site is the femur, with a pronounced predilection for the posterior aspect of the distal femoral shaft (7, 8). Ninety percent of parosteal osteosarcomas involve the metaphysis; two thirds are confined to the metaphysis. Diaphyseal involvement alone is seen in up to 10% of cases (9).

Clinically, parosteal sarcoma presents as a slowly growing painless mass, unless it is close to a joint, in which case the tumor may cause local tenderness with loss of range of motion (10). Biologically, it is a slowly progressive disease. Pulmonary metastases tend to appear late in the course of the disease, frequently following one or more local recurrences. Therefore, therapy is surgical, and is directed toward control of the primary tumor. Early diagnosis depends on clinical suspicion, thorough radiologic evaluation, and accurate histologic interpretation. Appropriate timely therapy usually presages a favorable prognosis (11).

The radiological appearance is well described in the literature. Radiographically, these tumors are eccentrically placed, lobulated, and densely mineralized. Parosteal osteosarcomas are attached to the underlying cortex by a broad base with a lucent zone, called the cleavage plane, between the underlying cortex and the tumor; however, this latter finding is not constant (3, 7).

Table. Clinical details, MRI signal intensity, and histopathological results

Case	Age/Sex	Site	Size	T1-signal intensity	T2-signal intensity	Hemorrhage/Necrosis	Grade
1	38/F	Femur, distal, posterior	19 cm	Hypo	Hyper-Heterogeneous	+	I
2	23/F	Femur, distal, posterior	4.5 cm	Hypo	Hyper	-	I
3	50/F	Humerus, proximal, anterior	8 cm	Hypo	Hyper-Heterogeneous	+	I
4	54/F	Femur, distal, posterior	15 cm	Hypo-Heterogeneous	Hyper-Heterogeneous	+	I
5	27/F	Tibia, proximal, posterior	10 cm	Hypo	Hyper	-	I
6	24/M	Femur, proximal, anterior	12 cm	Hypo	Hyper-Heterogeneous	+	I
7	17/F	Femur, distal, posterior	6.5 cm	Hypo	Hyper	-	II
8	34/F	Femur, proximal, posterior	6 cm	Hypo-Heterogeneous	Hyper-Heterogeneous	+	II
9	33/F	Femur, distal, posterior	7.5 cm	Hypo	Hyper-Heterogeneous	+	II
10	32/F	Femur, distal, posterior	9 cm	Hypo	Hyper-Heterogeneous	+	III
11	46/M	Femur, distal, posterior	25 cm	Hypo-Heterogeneous	Hyper-Heterogeneous	+	III
12	28/F	Femur, distal, posterior	10 cm	Hypo	Hyper-Heterogeneous	+	III

M: male, F: female

CT accurately defines the extent of the tumors for surgical planning, although tumor bone often cannot be distinguished from thickened host bone. CT cannot differentiate the lucent areas within dense tumors, which contain either benign tissue or tumor of any grade. CT may not reveal small satellite nodules beyond the main tumor (5). MRI is preferred for evaluation of bone marrow, and for identification of satellite lesions; CT is optimal for assessment of cortical integrity (2).

Histologically, there are long, narrow trabeculae or ill-defined islands of osteoid and woven bone separated by a fibrous stroma. The trabeculae may undergo maturation that results in the formation of normal-appearing lamellar bone. About 15% of tumors show high-grade components; low-grade tumors carry a significant risk of dedifferentiation to a high-grade sarcoma. Most commonly, dedifferentiation occurs by progressive malignant transformation of a low-grade tumor with loss of histologic differentiation, increased mitotic and growth rate, and metastatic spread (3, 12).

We had 6 Grade I, 3 Grade II, and 3 Grade III tumors. Grade III tumors were large masses, which may have been of lower grade when they first arose, but dedifferentiated over time. Ten patients presented to the orthopedics clinic with a palpable mass, the average size of which was significantly larger than those reported in the literature. Tumors that are large at presentation may have grown to encircle the underlying bone (13). On MRI, ossified components were of hypointense signal, and necrotic and hemorrhagic components were heterogeneously hyperintense on T2-weighted images.

The average sizes of Grade I, II, and III tumors were 11.3 cm, 6.6 cm, and 14.5 cm, respectively, indicating that in our small sample, there was not a simple relationship between tumor size and the histologic grade. In larger tumors, hyperintense areas of necrosis and haemorrhage occurred and these along with the hypointense (ossified) components caused a heterogeneous appearance, regardless of the grade of the tumor.

On MRI, parosteal osteosarcomas are hypointense on both T1- and T2-weighted images due to their dense osteoid components, especially in small tumors. Jelinek et al. suggest that low signal intensity on both T1- and T2-weighted images indicates a low-grade lesion; high signal intensity on T2-weighted images indicates a high-grade component (6). However, in this study, low-grade large masses also showed high signal intensity due to degeneration, hemorrhage, and necrosis. We could not correlate the high signal intensity with tumor grade. In a case study reported by Futani et al., T2-weighted images were not sufficient to differentiate the high-grade sarcomatous component, consistent with our findings (14).

In a review by Okada et al., the histologic diagnoses of the dedifferentiated components included fibroblastic osteosarcoma, fibrosarcoma, malignant fibrous histiocytoma, osteoblastic osteosarcoma, and chondroblastic osteosarcoma (15). Dedifferentiation is the development of a new high-grade malignancy in association with a preexisting low-grade malignancy or a benign tumor, and is not necessarily accompanied by necrosis and hemorrhage (15). Thus, high signal intensity on T2-weighted images of tumors of all grades does not necessarily identify a dedifferentiated component of the tumor. However, contrast-enhanced images may reveal the solid component in the heterogeneous areas on T2-weighted images, and can indicate the appropriate site for biopsy.

Opinions differ as to whether intramedullary extension has prognostic relevance. Campanacci et al. report that there is a strong relationship between the histologic grade and intramedullary extension, whereas Sheth et al. could not find any correlation (10,

16). Bertoni et al. showed that invasion of the medullary canal was more frequent in dedifferentiated parosteal osteosarcoma than in conventional osteosarcoma (65% vs. 28%) (17). Intramedullary extension was evident in 3 of the Grade I cases, 2 of the Grade II cases, and all of the Grade III cases in our study. The numbers are too limited to draw any conclusion in this regard; however, it is clear that MRI is capable of revealing subtle marrow changes.

Our study is limited by the relatively small number of cases of each subgroup. We also were not able to perform direct mapping of MRI findings with pathologic specimens.

In conclusion, the signal characteristics of parosteal osteosarcomas on MRI may vary in relation to the size of the tumor, as well as the presence of hemorrhage and necrosis. Therefore, MRI signal characteristics are not useful for tumor grading. The main advantage of MRI is that contrast-enhanced images may delineate the appropriate biopsy site. The effect of medullary invasion on the prognosis is controversial; however, MRI is the best imaging modality to assess medullary involvement, and can guide the surgical plan to ensure adequate resection of bone marrow infiltrated by tumor.

References

1. Wines A, Bonar F, Lam P, McCarthy S, Stalley P. Telangiectatic dedifferentiation of a parosteal osteosarcoma. Skeletal Radiol 2000; 29:597–600.
2. Yu JS, Weis LD. MR imaging of parosteal osteosarcoma in two skeletally immature patients. Clin Imaging 1997; 21:63–68.
3. Shuhaibar H, Friedman L. Dedifferentiated parosteal osteosarcoma with high-grade osteoclast-rich osteogenic sarcoma at presentation. Skeletal Radiol 1998; 27:574–577.
4. Jee WH, Choe BY, Ok IY et al. Recurrent parosteal osteosarcoma of the talus in a 2-year-old child. Skeletal Radiol 1998; 27:157–160.
5. Hudson TM, Springfield DS, Benjamin M, Bertoni F, Present DA. Computed tomography of parosteal osteosarcoma. AJR Am J Roentgenol 1985; 144:961–965.
6. Jelinek JS, Murphey MD, Kransdorf MJ, Shmookler BM, Malawer MM, Hur RC. Parosteal osteosarcoma: value of MR imaging and CT in the prediction of histologic grade. Radiology 1996; 201: 837–842.
7. Abdelwahab IF, Kenan S, Hermann G, Klein MJ. Dedifferentiated parosteal osteosarcoma of the radius. Skeletal Radiol 1997; 26: 242–245.
8. Chew FS, Richardson ML. A benign appearing bone mass. AJR Am J Roentgenol 2005; 184:S169–S174.
9. Partovi S, Logan PM, Janzen DL, O'Connell JX, Connell DG. Low-grade parosteal osteosarcoma of the ulna with dedifferentiation into high-grade osteosarcoma. Skeletal Radiol 1996; 25:497–500.
10. Campanacci M, Picci P, Gherlinzoni F, Guerra A, Bertoni F, Neff JR. Parosteal osteosarcoma. J Bone Joint Surgery Br 1984; 66:313–321.
11. Lindell MM, Shirkhoda A, Raymond AK, Murray JA, Harle TS. Parosteal osteosarcoma: radiologic-pathologic correlation with emphasis on CT. AJR Am J Roentgenol 1987; 148:323–328.
12. Takeuchi K, Morii T, Yabe H, Morioka H, Mukai M, Toyama Y. Dedifferentiated parosteal osteosarcoma with well-differentiated metastases. Skeletal Radiol 2006; 35:778–782.
13. Tigges S, Erb RE, Nance EP. Skeletal case of the day. AJR Am J Roentgenol 1992; 158:1368.
14. Futani H, Okayama A, Maruo S, Kinoshita G, Ishikura R. The role of imaging modalities in the diagnosis of primary dedifferentiated parosteal osteosarcoma. J Orthop Sci 2001; 6:290–294.
15. Okada K, Frassica FJ, Sim FH, Beabout JW, Bond JR, Unni KK. Parosteal osteosarcoma. A clinicopathological study. J Bone Joint Surgery Am 1994; 76:366–378.
16. Sheth DS, Yasko AW, Raymond AK et al. Conventional and dedifferentiated parosteal osteosarcoma. Diagnosis, treatment and outcome. Cancer 1996; 78:2136–2145.
17. Bertoni F, Bacchini P, Staals EL, Davidovitz P. Dedifferentiated parosteal ostesarcoma: the experience of the Rizzoli Institute. Cancer 2005; 103:2373–2382.